Detection the Urban Changing Areas of Yangon City Using Landsat Time series Images

Thida Aung and Myint Myint Sein
tdathida@ucsy.edu.mm,myint@ucsy.edu.mm

Abstract

Urban growth is the critical task for city planning of the developing country. It can estimate to know the increasing rate of the building area of the certain township during the specific year. The system proposes a method combining the Morphological Building Index (MBI) and Slow Feature Analysis (SFA). It can find the urban changing areas of the Yangon city using the Landsat 7 ETM$^+$ time series images from 2003 to 2015. In MBI, it leads to a number of false alarms involving non-building urban structures such as soil and roads. In SFA, it alone is not suitable for building change detection since it provides high commission error. The purposed system combines these two method to overcome the weakness of MBI and SFA. The experimental result shows the comparative accuracies of MBI and SFA method only with the proposed method.

Keywords: Morphological Building Index, Slow Feature Analysis, Landsat

1. Introduction

Urban growth is the global effect and urbanization is more rapid in the developing country in recent year. Estimating the urban growth is the critical task for managing natural resources and monitoring the environmental changes. Urbanization is the migration from a rural to an urban society, bringing a large concentration of people into towns and cities. This process usually occurs when a nation is still developing. Urban growth is based on the change detection of the satellite images such as Landsat, SPOT images, ASTER images, GeoEye images, DigitalGlobe images and so on. Change detection technique is a process that analyses the pair of images taken at different time to identify the changes of the specific area. It is now feasible to provide consistent monitoring of landscape conditions, such as land-use/land-cover change, ecosystem monitoring, urban expansion, resource management, and disaster assessment. So it need to develop the effective change detection technique for the better accuracy. [1] A large variety of building detection techniques and algorithms have been reported in the literature, but most detection algorithms rely on edge-based techniques that consist of linear feature detection, grouping for parallelogram structure extraction, and building polygons verification using knowledge such as geometric structure, shadow, and so forth. In order to solve this complex problem, integrating the power of multiple algorithms, cues, and available data sources is also implemented recently to improve the reliability and robustness of the extraction results.

Recent researches in this area focus on automatic and unsupervised extraction of urban area. Hafez. Afify proposed to assess, evaluate and monitor the nature and extent of land cover change in New Burg El-Arab city through the period from 1990 to 2000 using remotely sensed Landsat multispectral images. [2]

W. Jie, L. Congcong, H. Luanyun, Z. Yuanyuan, H. Huabing and G. Peng proposed an approach to map dynamic land cover types with frequently available satellite data. Landsat 8 data acquired from nine dates over Beijing within a one-year period were used to map seasonal land cover dynamics. A Markov random field (MRF) model was applied to maintain the spatio-temporal consistency. This system is based on supervised classification on nine data set on the Landsat 8 images. So it takes more time for preparing training data sets and classification method. [3] In practice, the temporal spectral variance makes it difficult to separate changes and non-changes.

W. Chen, D. Bo propose a novel slow feature analysis (SFA) algorithm for change detection. Compared with changed pixels, the unchanged ones should be spectrally invariant and varying slowly across the multi-temporal images. In this paper, SFA extracts the most temporally invariant component from the multi-temporal images to transform the data into a new feature space. It is not only related to the change of buildings, but also to other urban structures. [4]

This paper is organized as follows: The system overview is discussed in section 2 and Methodology is expressed in Section 3. In section 4, experiments can be seen and section 5 gives the discussion and conclusion

2. Overview the System

The purpose system is divided into three parts. They are 1) input images 2) preprocessing stages that contains TOA radiance calculation 3) Perform SFA and MBI 4) Combine SFA and MBI 5) Output the change results as shown in Figure 1.

3. System Methodology

It contains three parts: Preprocessing Method for Landsat images, Slow Feature Analysis (SFA) and Morphological Building Index (MBI).

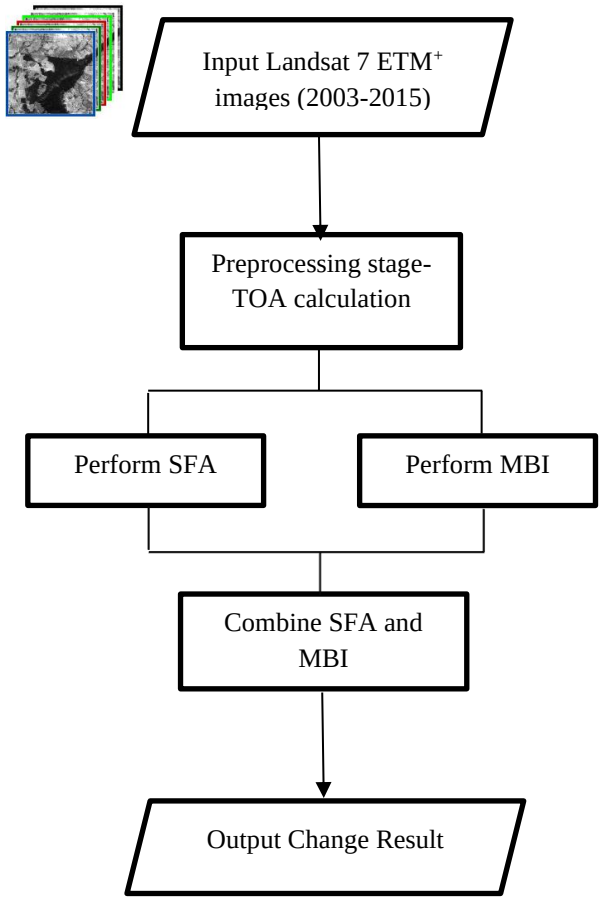

Figure 1: System Flow Diagram

3.1. Preprocessing Method for Landsat Times Series Images - TOA Radiance Calculation

Landsat data from the USGS were already radiometrically and geographically corrected, but fitted in 8 bit files (ranges from 0 to 255). In other terms, each image was matrix of DNs (Digital Numbers) while to calculate vegetation indices, reflectance values (physical measurements of the part of the solar energy reflected by earth features) were required [5], [6]. At first DNs were transformed to radiance using the formula:

$$L_\lambda = (gain*DN) + bias_\lambda \quad (1)$$

L_λ is the calculated radiance associated to the ground area enclosed in the pixel and referred to the λ wavelength range of the specific band; DN is the digital number of the pixel of the Landsat 7 ETM+ band image; gain and $bias_\lambda$ are sensor-specific calibration parameters determined before the launch.

In Table 1 gain and bias values for bands used in this application and given in Chander et al [7] are reported.

TABLE 1. Gain and Bias for 3 and 4 bands

Spectral Band	Gain	$Bias_\lambda$
Band 3	0.621654	-5.62
Band 4	0.639764	-5.74

The resulting radiance was the quantity measured by the Landsat sensor without consideration of the position of the sun and the differing amounts of energy output by the sun in each band. The fraction of the sun's energy that is reflected by the surface at specific wavelength values. In this application Top-Of-Atmosphere (TOA) reflectance was considered: it represents the solar radiation incident on the satellite sensor in standard unit less terms, independent of the position of the sun with respect to the earth. TOA is not the reflectance that would be recorded by a hand-held spectrophotometer on the ground because of the atmospheric effects. In fact the electromagnetic radiation incident on the satellite sensor is significantly distorted by interaction with gases and aerosols in the earth's atmosphere, both on the way down to the ground, and once more on the way back up to the instrument. Nevertheless using TOA values rather than DNs better results are achieved. [11]

In this application at-sensor radiance values were converted to TOA reflectance values using the following formula:

$$R_\lambda = \frac{\pi . L_{,\lambda} . d^2}{E_{sun,\lambda} . \sin \theta_{SE}} \quad (2)$$

where R_λ is the reflectance (unitless ratio) referred to the λ wavelength range of the specific band; L_λ is the radiance calculated by formula 1; d is the earth-sun distance (in astronomical units); $E_{sun,\lambda}$ is the mean exoatmospheric solar irradiance at the specific band; sin θ_{SE} is the solar elevation angle. Values of $E_{sun,\lambda}$ were achieved by Chander et al article and reported in Table 2 for the two bands of interest.

Table 2. Specific Radiance of Sun in band 3 and band 4

Spectral Band	Sun Radiance Esun,λ [Watts/(sq. meters·μm)]
Band 3	1533
Band 4	1039

Values of d and sin θ_{SE} were established in consideration of their dependence by the day of the year and the time of day when the scene was captured. Specifically θ_{SE} was already indicated in the metadata file with the images, while d was derived from tabulates of the Nautical Almanac (United States Naval Observatory) [12] in consideration of the acquisition day (DOY= day of the year=121; d=1.00756 astronomical units).

3.2. Morphological Building Index (MBI)

Computation of MBI can be briefly expressed as the following steps:

Step1: Brightness image

The maximum value of the visible bands for each pixel i is recorded as the brightness b (i):

$$b(i) = \max_{1 \le k \le K} (band_k(i)) \quad (3)$$

where band $band_k(i)$ indicates the digital number (DN) value for pixel i for the k^{th} visible band. K is the total number of the visible spectral bands.

Step 2: Differential top-hat profiles (DTPs)

DTPs are constructed using a series of multi-scale and multidirectional linear structural elements (SEs) to represent the high local contrast of buildings:

$$DTP\ (d,s) = |TH_I(\mathrm{d}, \mathrm{s}+\Delta\mathrm{s}) - TH_I(\mathrm{d}, \mathrm{s})| \quad (4)$$

where s and d indicate the length and direction of the linear SE, respectively, and Δs is the increment of the length. THI (d, s + Δs) and THI (d, s) represent the top-hat-by-reconstruction of the brightness image I with a linear SE of length (s + Δs) and s, respectively. It should be noted that a linear SE is able to measure the directionality of a structure and, hence, has potential for discrimination between buildings (isotropy) and roads (anisotropy).

Step 3: Calculation of MBI

$$\mathrm{MBI} = \frac{\sum_{\mathrm{d,s}} \mathrm{DTP(d,s)}}{\mathrm{D}*\mathrm{S}} \quad (5)$$

where D and S are, respectively, the number of directions and number of lengths considered for the DTPs. According to our previous experiments, four directions (D = 4) are adequate for describing the geometrical attributes of buildings. The scale parameter **s** is determined according to the sizes of the buildings and the spatial resolution of the specific image considered.

3.3. Slow Feature Analysis (SFA)

Given a bi-temporal spectral vector pair $x^i = [x_1^i, \ldots, x_N^i]$ and $y^i = [y_1^i, \ldots, y_N^i]$, where i indicates the pixel number and N is the dimension of the band, the input is normalized with zero mean and unit variance, expressed as equation (6) and (7);

$$\hat{x}_j^i = \frac{x_j^i - \mu_{x_j}}{\sigma_{x_j}} \quad (6)$$

$$\hat{y}_j^i = \frac{y_j^i - \mu_{y_j}}{\sigma_{y_j}} \quad (7)$$

where μ_{x_j} is the mean and σ_{x_j} is the variance for band j of image X.

The SFA algorithm is reformulated with the normalized multi temporal pairs and rewrite in equation (8) as

$$\frac{1}{P}\sum_{i=1}^{P} (g_j(\hat{x}^i) - g_j(\hat{y}^i))^2 \text{ is minimal} \quad (8)$$

where P is the number of bitemporal spectral vector pairs in the input data set.[8]

The constraints of original SFA are written in equation (9), (10) and (11) by replacing the time series with the average over the data set of the bi temporal pairs.

$$\frac{1}{2P}[\sum_{i=1}^{P} g_j(\hat{x}^i) + \sum_{i=1}^{P} g_j(\hat{y}^i)] = 0 \quad (9)$$

$$\frac{1}{2P}[\sum_{i=1}^{P} g_j(\hat{x}^i)^2 + \sum_{i=1}^{P} g_j(\hat{y}^i)^2] = 1 \quad (10)$$

$$\frac{1}{2P}[\sum_{i=1}^{P} g_j\left(\hat{x}^i\right) g_l\left(\hat{x}^i\right) + \sum_{i=1}^{P} g_j(\hat{y}^i) g_l(\hat{y}^i)] = 0 \quad (11)$$

The optimization problem can be written as

$$\frac{1}{P}[\sum_{i=1}^{P} \left(\hat{x}^i - \hat{y}^i\right)\left(\hat{x}^i - \hat{y}^i\right)^T = \sum_{\Delta} = \mathrm{A} \quad (12)$$

$$\frac{1}{2P}[\sum_{i=1}^{P} \left(\hat{x}^i\right)\left(\hat{x}^i\right)^T + \sum_{i=1}^{P} \left(\hat{y}^i\right)\left(\hat{y}^i\right)^T = \frac{1}{2}(\sum_x + \sum_y) = \mathrm{B} \quad (13)$$

where $\sum_{\Delta}$ is the covariance matrix of the temporal difference and $\sum_x$, $\sum_y$ is the covariance matrix of each bitemporal input.

With (12) and (13) can be reconstructed as

$$\frac{w_j^T A w_j}{w_j^T B w_j} = \frac{w_j^T \sum_{\Delta} w_j}{w_j^T \frac{1}{2}(\sum_x + \sum_y) w_j} \quad (14)$$

Essentially, (14) means that the SFA change detection algorithm aims to find a function that obtains the lowest covariance of the difference values between the temporally invariant samples across different times while containing the most information.[6]
A transformation matrix can be obtained to solve the eigenvalue problem. In the transformed difference space, the unchanged samples will be suppressed, and hence, the separation between the changes and non-changes will be strengthened. Finally, the SFA variable shown in equation (15) is computed as

$$SFA_j = w_j \hat{x} - w_j \hat{y} \quad (15)$$

4. Experimental Result

4.1. Data Sets

The Landsat Program is a joint effort of the U.S. Geological Survey (USGS) and the National Aeronautics and Space Administration (NASA) to regularly acquire land imagery from space. Landsat 7 satellite, launched on April 15, 1999, is still operational: moving in a descending orbit (from north to south) over the sunlit side of the Earth at 705 kilometers (438 miles) altitude, it makes a complete orbit every 99 minutes, completes about 14 full orbits each day, and crosses every point on Earth once every 16 days.[7]

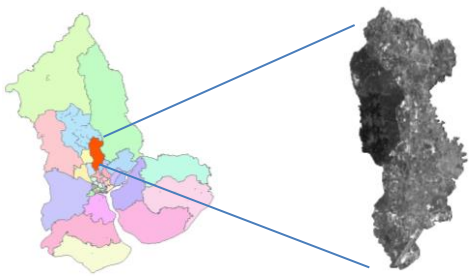

Figure 2: Area of Interest, Mingalardon Township

One scene of multispectral Landsat Thematic Mapper (TM) image covering the entire Mingalardon Township area was used as data source in this study. This image has seven spectral bands with 30-m spatial resolution, and was acquired on January 1, 2003. The Area of Interest (AOI) was subsetted by the administrative vector boundary of Mingalardon Township (106.6 km^2) of Yangon city, which is shown in Figure 2.

4.2. Results

The system takes the landsat images of 10 years from 2003 to 2015. After inputting the images the system converts Digital Number (DN) to reflectance value. This stage is needed for removing the inconsistent of the input images caused by atmospheric condition, sun reflectance. The output bands of preprocessing stage are shown in figure 3.

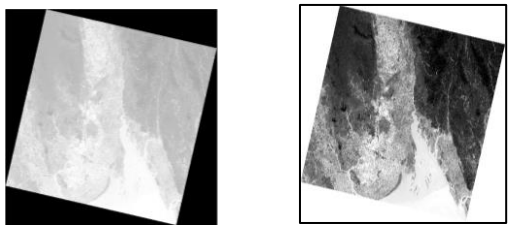

(i) Original Band 3 (ii) Reflectance output of Band 3

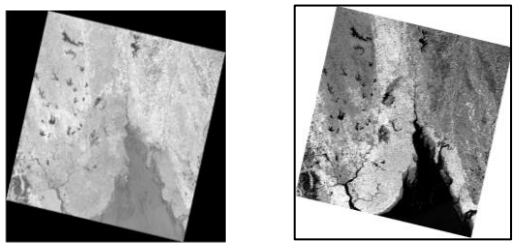

(iii) Original Band 6 (ii) Reflectance output of Band 6

Figure 3: Output of preprocessing step

Morphological Building Index (MBI), it leads to a number of false alarms involving non-building urban structures such as soil and roads. Its accuracy is relates to the radiometric conditions of the image. [18]

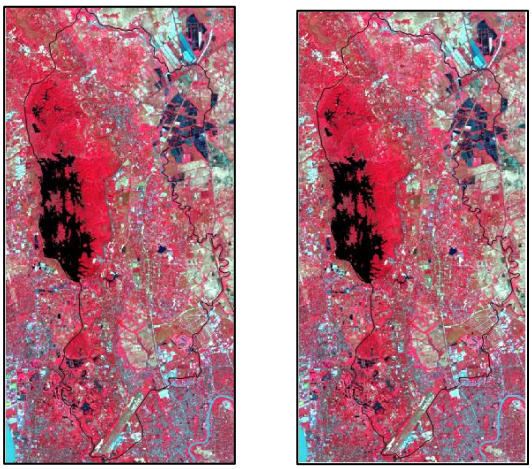

(i) 2013 (ii) 2015

Figure 4: Color Composite Change Map of 2013 and 2015

In Slow Feature Analysis (SFA), it alone is not suitable for building change detection since it provides high commission error. It is not only related to the change of buildings, but also to other urban structures. So the result of MBI and SFA are compared to detect the change of the damage areas. Decreasing damage building area are estimated by comparing with *MBI (t2)* and *SFA*. *MBI (t1)* and *MBI (t2)* represents building components extracted by *MBI* for time *t1* and *t2*, respectively.

Three indices are used to assess the results: correctness, completeness, and quality shown in Figure 5.

$$Correctness = \frac{TP}{TP + FP}$$

$$Completeness = \frac{TP}{TP + FN}$$

$$Quality = 100 * \frac{TP}{TP + FN + FP}$$

where TP (true positive) are the numbers of changed pixels in the result, but correctly changed in the reference image. FP (false positive) are the changing pixels in the result, but not change in the reference image. TP and FP are counted inside the Mingalardon Township administrative boundary. FN (false negative) is the number of changed pixels in the reference image, but detected as unchanged in the result.

The correctness, completeness and quality of MBI are derived from [10]. This system works on both of the low and high resolution of the input images.

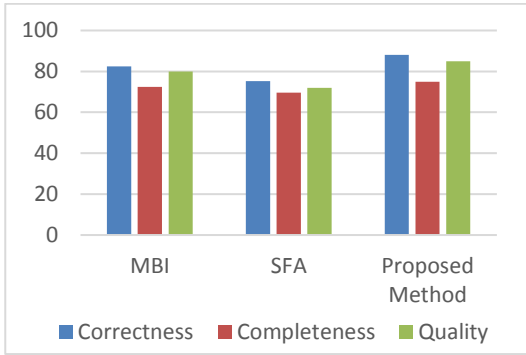

Figure 5: Quantitative comparison of the proposed method

5. Conclusion

The changing areas of the urban region are automatically extracted by combination of MBI and SFA method. Since the purposed method uses unsupervised technique, the training data is not required. So it can save the time for the training samples than other supervised method. In the proposed system, it also needs the some better preprocessing step for the satellite images. This system uses TOA rather than ground level reflectance, so acceptable results can be achieved. Besides this system detects the urban changing area based on the indices from combing SFA and MBI. But it only calculates the urban built-up area

of the specific region. In the future, complete preprocessing steps such as geometric correction, atmospheric correction and removing cloud coverage will be performed and decreasing rate of building areas can be analyzed for the Landsat time series images. This system will be proposed to detect the damage area of the specific region taking the before and after images when the disaster is happened. [8, 9]

References

[1] O. Aytekin, A. Erener, I. Ulusoy, S. Duzgun," Unsupervised building detection in complex urban environments from multispectral satellite imagery", International Journal of Remote Sensing, April, 2012,2152-2177

[2] H. A. Afify, "Evaluation of change detection techniques for monitoring land-cover changes: A case study in new Burg El-Arab area", Alexandria Engineering Journal, Egypt, 2011, pp.187–195.

[3] W. Jie, L. Congcong, H. Luanyun, Z. Yuanyuan, H. Huabing, G. Peng, "Seasonal Land Cover Dynamics in Beijing Derived from Landsat 8 Data Using a Spatio-Temporal Contextual Approach", Remote Sensing Journal, China, 2015, 7, pp. 865-881.

[4] W. Chen, D. Bo, "Slow Feature Analysis for Change Detection in Multispectral Imagery", IEEE Transaction on Geoscience and Remote Sensing Journal, 2013.

[5] G. J. Firl, L. Carter, and Lesson 10: Calculating Vegetation Indices from Landsat 5 TM and Landsat 7 ETM+ Data, Colorado State University, 2013.

[6] X. Chen, L. Vierling, D. Deering, "Simple and effective radiometric correction method to improve landscape change detection across sensors and across time", Remote Sensing of Environment, Vol. 98, 2005, pp. 63– 79.

[7] G. Chander, B. L. Markham, and D. L. Helder, "Summary of current radiometric calibration coefficients for Landsat MSS, TM, ETM+, and EO-1 ALI sensors", Remote Sensing of Environment, Vol. 113, 2009, pp. 893-903.

[8] A. Thida, K. C. Moe, M. M. Sein, "Change Detection of the Building areas in Urban Regions", in Proceedings of the 14th International Conference on Computer Applications (ICCA2016), pp. 124-130, February 2016, Yangon.

[9] A. Thida, M. M. Sein, "Analysing the Effect of Disaster", in Proceedings of the 10th International Conference on Genetic and Evolutionary Computing (ICGEC), November, 2016, China.

[10] K.C.Moe and M.M.Sein, "Urban Growth Detection using Morphology of Satellite Image," in Proceedings of International Conference on Science, Technology, Engineering and Management (ICSTEM,2015), ISBN: 978-93-84209-89-6, pp. 43-47, Singapore, February 2015

[11] R Irish, "Calibrated Landsat Digital Number (DN) to Top of Atmosphere (TOA) Reflectance Conversion", Remote Sensing Basics, August, 19 2008.

[12] Nautical Almanac Office. The Nautical Almanac for the Year, United States Naval Observatory, Washington, DC: U.S. Government Printing Office.